J. Fluid Mech. (1981), *vol.* 111, *pp.* 107–122
Printed in Great Britain

The early stages of contaminant dispersion in shear flows

By RONALD SMITH
Department of Applied Mathematics and Theoretical Physics,
University of Cambridge

(Received 1 November 1980)

The dispersion of a spot of contaminant in a high-Péclet-number laminar flow is studied by means of the ray method developed by Cohen & Lewis (1967). This method is free from the usual severe restrictions on the time range. Thus, it is possible to investigate strong shear-distortions of the concentration distribution. Also, the effects of rigid boundaries can be allowed for simply by including reflected rays. Three examples are studied in detail: stagnation flow, a point vortex and plane Poiseuille flow.

1. Introduction

The dispersion of a point source of contaminant in a laterally confined flow can be regarded as being comprised of three stages (see figure 1). Initially the contaminant distribution spreads out symmetrically by molecular diffusion and is carried along at the local fluid velocity. Then, as the contaminant cloud becomes larger, it extends over a range of velocities and is pulled out into a highly elongated shape. Finally, the contaminant cloud extends right across the flow and the residual cross-stream concentration variations have the same general shape as the velocity profile.

Following upon G. I. Taylor's seminal ideas (Taylor 1953, 1954), most theoretical investigations of contaminant dispersion have been concerned with the large-time behaviour. However, for some applications, as diverse as arterial blood flow (Caro 1966), and the flow of the Mississippi river (McQuivey & Keefer 1976*b*), there is insufficient time for cross-sectional mixing to be achieved. This has led to the development of heuristic approximations (Gill & Sankarasubramanian 1970; McQuivey & Keefer 1976*a*; Smith 1981) and to rigorous analyses of the small-time behaviour (Lighthill 1966; Chatwin 1976, 1977; Barton 1978).

The range of validity for the rigorous analyses is extremely restricted. For Poiseuille pipe flow, this is because Lighthill's remarkable exact analytic solution does not include the effects either of longitudinal diffusion or of the walls. In the more universally applicable work of Chatwin and of Barton, the restrictions arise because of the need to represent the local velocity field by a Taylor series expansion. Thus, the contaminant cloud cannot have grown to a size comparable with the dimensions of the flow and cannot have advected into a region of different velocity from the velocity at the source (i.e. figure 1 (i), as opposed to figure 1 (ii)).

The purpose of the present paper is to give a solution for the contaminant distribution which is free from these restrictions and therefore encompasses the régime shown in figure 1 (ii). Instead of making an expansion for small times, we give an expansion for large Péclet numbers (i.e. a Reynolds number for diffusion with the

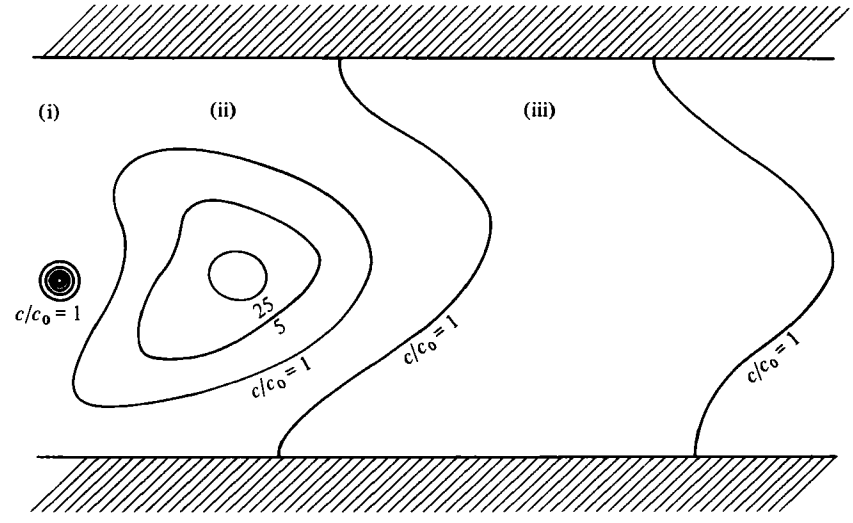

FIGURE 1. Sketch of concentration contours in the early (i), moderate (ii), and late (iii) stages of contaminant dispersion.

diffusivity of mass replacing that of momentum). The mathematical groundwork was done by Cohen & Lewis (1967), and the rigorous validity of the method proved by Cohen, Hagin & Keller (1972). The idea is that, by analogy with the role of group-velocity paths in wave problems, there are 'ray' directions for the transmission of information in diffusion problems. Thus, to construct the concentration distribution it is first necessary to determine the ray paths, then to evaluate the transmitted information, and hence to determine the concentration. One convenient feature of the method is that to include the effect of walls it suffices that rays are reflected, with the angle of incidence equal to the angle of reflection.

After the present work had been completed, it was learned that the relevance of Cohen & Lewis's method to advection–diffusion had been recognized over ten years ago by Albion D. Taylor (unpublished manuscript†). The problem addressed by Taylor is totally general and includes non-constant anisotropic diffusion, unsteady compressible flows, and the calculations are carried out to arbitrarily high order. The present work can be regarded as being a demonstration that it is a practicable proposition to apply Taylor's ideas to specific flows. A copy of Taylor's manuscript was provided by a referee, and at his suggestion has been lodged with the editor for inspection.

2. Ray expansion

There are very few flows for which there are exact solutions of the unsteady advection–diffusion equation

$$\partial_t c + \mathbf{u}.\nabla c = P^{-1}\kappa\nabla^2 c. \tag{2.1}$$

Here $c(\mathbf{x},t)$ is the concentration, $\mathbf{u}(\mathbf{x})$ the steady laminar flow velocity, ∇ the three-dimensional gradient operator, κ the constant diffusivity, and P the Péclet number.

† This paper is available from the editorial office of the *Journal of Fluid Mechanics*.

The exact solutions are either already exponential (Townsend 1951; Lighthill 1966; Chatwin 1974), or asymptote to exponentials when P is large (Cohen & Lewis 1967). Thus, when seeking asymptotic solutions, it is convenient to build in this structure *a priori* (Cohen & Lewis 1967, equation (5.2.2)):

$$c = A \exp(\pm P\phi). \tag{2.2}$$

Here A is an amplitude factor and ϕ the decay exponent. The $\pm$ sign is a technical device to ensure that the auxiliary functions preserve the physically correct symmetry with respect to reversal of the advective rate of change $\pm(\partial_t + \mathbf{u}.\nabla)$.

If we substitute the *ansatz* (2.2) into (2.1) and collect $\exp(\pm P\phi)$ and $\pm\exp(\pm P\phi)$ terms separately, then we find

$$(\partial_t + \mathbf{u}.\nabla)\phi = \kappa(\nabla\phi)^2 + P^{-2}\kappa\nabla^2 A, \tag{2.3}$$

$$(\partial_t + \mathbf{u}.\nabla)A = \kappa\nabla.(A\nabla\phi) + \kappa\nabla\phi.\nabla A. \tag{2.4}$$

Although it is not justifiable to delete the P^{-1} diffusive term in (2.1), it is justifiable to neglect the P^{-2} term in (2.3). The reason for this is that the concentration is a rapidly varying function of position, but by means of the nonlinear transformation (2.2), we have changed dependent variables to the gradually varying auxiliary functions A, ϕ. Thus, in (2.3) the presence of the small parameter P^{-2} genuinely means that the corresponding term is negligible.

We record that the splitting (2.3), (2.4) into two equations is not unique. For example, Cohen & Lewis (1967, equations (3.1.2), (3.1.3)) use the decomposition

$$(\partial_t + \mathbf{u}.\nabla)\phi = \kappa(\nabla\phi)^2, \tag{2.5}$$

$$(\partial_t + \mathbf{u}.\nabla)A = \kappa\nabla.(A\nabla\phi) + \kappa\nabla\phi.\nabla A + P^{-1}\kappa\nabla^2 A. \tag{2.6}$$

The leading-order terms are the same as in (2.3) and (2.4). However, if higher-order corrections are sought, then the present approach is preferable in that the expansion proceeds as P^{-2} and not as P^{-1}.

3. Ray tracing

In the terminology of ray methods, (2.3) with the $P^{-2}\nabla^2 A$ term neglected, is called the 'eikonal' equation. This equation is a nonlinear first-order partial differential equation and can be solved by the method of characteristics (Courant & Hilbert 1962, chapter 2). The characteristic or ray velocity is given by

$$\mathbf{R} = \mathbf{u} - 2\kappa\nabla\phi, \tag{3.1}$$

and the characteristic equations are

$$dt/ds = 1, \quad d\mathbf{x}/ds = \mathbf{R}, \tag{3.2}$$

where s is a parameter along the rays. The crucial feature is that along the rays the partial differential equation (2.3) turns into an ordinary differential equation

$$d\phi/ds = -(\mathbf{u} - \mathbf{R})^2/4\kappa. \tag{3.3}$$

Thus, the rate of exponential decay of the concentration depends upon the magnitude of the difference between the local velocity and the ray velocity.

The complete characteristic system of equations (Courant & Hilbert, chapter 2, § 7, equation (2)), includes in addition to equations (3.2), (3.3), equations for the rates of change of $\partial_t \phi$ and $\nabla\phi$ along rays. The first of these yields a ray invariant

$$\partial_t \phi = \text{constant along rays}, \tag{3.4}$$

and the second can be more usefully cast as an equation for the rate of change of $\mathbf{R}$:

$$d\mathbf{R}/ds = \nabla(\tfrac{1}{2}\mathbf{u}^2) - \mathbf{R}_\times(\nabla_\times \mathbf{u}). \tag{3.5}$$

Thus, when $\mathbf{R}$ is relatively small, the rays are primarily refracted towards regions of stronger current, and when $\mathbf{R}$ is large (i.e. the tails of the concentration distribution) the rays tend to rotate in the same sense as the vorticity.

Comparison of (3.5) with the identity

$$(\mathbf{u}.\nabla)\,\mathbf{u} = \nabla(\tfrac{1}{2}\mathbf{u}^2) - \mathbf{u}_\times(\nabla_\times \mathbf{u}), \tag{3.6}$$

enables us to infer that if initially $\mathbf{R} = \mathbf{u}$, then the ray continues to move with the fluid for all time. Equivalently, in the limit of large Péclet number, the centre of the contaminant distribution, where $\nabla\phi = 0$, is advected with the fluid velocity.

4. Transport equation

Not only does the eikonal equation turn into an ordinary differential equation along ray paths, but so also does the 'transport' equation (2.4):

$$dA/ds - A\kappa\nabla^2\phi = 0. \tag{4.1}$$

As if this was not enough good fortune, we can solve this equation without the need to evaluate the second derivative $\nabla^2\phi$ (Cohen & Lewis 1967, equation (5.2.17)).

To do this we introduce a set of ray parameters $\mathbf{p}$ (for example the initial value of $\mathbf{R} - \mathbf{u}$) and consider the ray separation

$$J = \partial(t, \mathbf{x})/\partial(s, \mathbf{p}). \tag{4.2}$$

Making repeated use of the chain rule

$$\partial^2\mathbf{x}/\partial p\,\partial s = (\partial\mathbf{x}/\partial p\,.\nabla)\,\partial\mathbf{x}/\partial s, \tag{4.3}$$

we can derive the relation

$$dJ/ds = J\nabla.\mathbf{R} = -2\kappa J\nabla^2\phi. \tag{4.4}$$

An immediate implication is that

$$AJ^{\frac{1}{2}} = \text{constant along rays}. \tag{4.5}$$

Hence, the greatest concentrations are to be determined where the rays are closest together.

To evaluate the ray constants in (3.4) and (4.5), we examine the solution very close to the source. For sufficiently short times the non-uniformity of the velocity field can be neglected and we have the elementary solution

$$c = \frac{P^{\frac{1}{2}n}}{[4\pi\kappa(t-t_0)]^{\frac{1}{2}n}} \exp\left[-\frac{P(\mathbf{x}-\mathbf{x}_0-\mathbf{u}_0(t-t_0))^2}{4\kappa(t-t_0)}\right], \tag{4.6}$$

with $n = 2, 3$ depending upon the dimensionality of the source. If $\mathbf{R}_0$ denotes the initial value of the ray velocity, then locally we have

$$\mathbf{x} = \mathbf{x}_0 + \mathbf{R}_0 s, \quad t - t_0 = s, \tag{4.7a, b}$$

$$\phi = -(t - t_0)(\mathbf{R}_0 - \mathbf{u}_0)^2/4\kappa, \tag{4.7c}$$

$$A = P^{\frac{1}{2}n}/[4\pi\kappa s]^{\frac{1}{2}n}. \tag{4.7d}$$

Hence we infer that $\phi = 0$ at the source, and we can evaluate the ray constants

$$\partial_t \phi = -(\mathbf{R}_0 - \mathbf{u}_0)^2/4\kappa \quad \text{along rays}, \tag{4.8}$$

$$AJ^{\frac{1}{2}} = \lim_{s \to 0} \{P^{\frac{1}{2}n} J^{\frac{1}{2}}/[4\pi\kappa s]^{\frac{1}{2}n}\} \quad \text{along rays}. \tag{4.9}$$

5. Reflection at boundaries

In wave problems, boundaries can be dealt with simply by the inclusion of reflected waves. Here we show that the same is true for the ray solution of a diffusion equation. The most commonly occurring boundary conditions are that either the contaminant flux or the concentration be zero. To include both these limits we investigate the slightly more general boundary condition

$$\mathbf{n} \cdot (\mathbf{u}c - P^{-1}\kappa \nabla c) - \beta c = 0 \quad \text{on} \quad \partial\Omega. \tag{5.1}$$

Here $\mathbf{n}$ is the outward normal, and β a reaction coefficient.

To solve (2.1) with the boundary condition (5.1), we pose the *ansatz*

$$c = A_I \exp(P\phi_I) + A_R \exp(P\phi_R). \tag{5.2}$$

In order to match the rapidly varying exponential decay rates we must have

$$\phi_I = \phi_R \quad \text{on} \quad \partial\Omega. \tag{5.3}$$

This applies whatever the boundary conditions. For the amplitude factors we have the problem-specific conditions

$$[\mathbf{n} \cdot (\mathbf{u} - \kappa \nabla \phi_I) - \beta] A_I + [\mathbf{n} \cdot (\mathbf{u} - \kappa \nabla \phi_R) - \beta] A_R = 0 \quad \text{on} \quad \partial\Omega, \tag{5.4}$$

where we have neglected terms of order P^{-1}.

Along rays the eikonal equation takes the form

$$(\mathbf{u} - 2\kappa \nabla \phi)^2 = \mathbf{u}^2 - (\mathbf{R}_0 - \mathbf{u}_0)^2, \tag{5.5}$$

where we have made use of the ray invariant (4.8). Geometrically, this can be interpreted as constraining the gradient vector $2\kappa\nabla\phi$ to a circle with centre $\mathbf{u}$, and with the ray velocity $\mathbf{R}$ directed towards the centre of the circle (see figure 2). At the boundary, the values of $\partial_t \phi$ are the same for both the incident and reflected rays. Thus, the invariant (4.8) is preserved under reflection and the circle radius in (5.5) is the same for the two rays. Also, the condition (5.3) implies that the components of $\nabla\phi$ along the boundary are the same for the two rays. This has the geometrical consequence that the ray direction is reflected at the boundary with the angle of incidence equal to the angle of reflection (see figure 2).

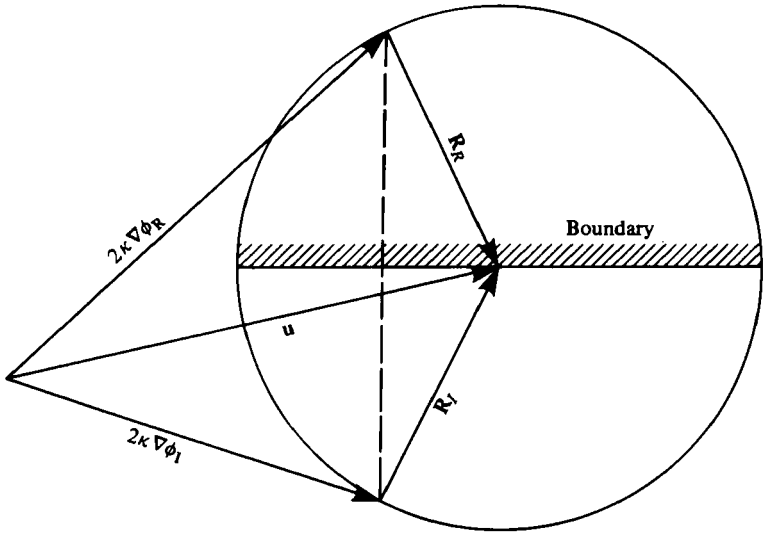

FIGURE 2. Geometrical interpretation of the eikonal equation, showing the relationship between incident and reflected rays at a boundary.

The contaminant flux velocity can be written as the mean value of the flow velocity and the ray velocity:

$$\mathbf{u}-\kappa\nabla\phi = \tfrac{1}{2}(\mathbf{u}+\mathbf{R}). \tag{5.6}$$

Since $\mathbf{R}$ reflects normally at the boundary, the amplitude boundary condition (5.4) becomes

$$A_R = A_I[\mathbf{n}.\mathbf{R}_I-(2\beta-\mathbf{u}.\mathbf{n})]/[\mathbf{n}.\mathbf{R}_I+(2\beta-\mathbf{u}.\mathbf{n})]. \tag{5.7}$$

Thus, if the reaction coefficient β exceeds half the suction velocity $\mathbf{u}.\mathbf{n}$, then for all rays the reflected amplitude is less than the incident amplitude. In the important limiting case of a non-reacting boundary with zero suction we have equality between the reflected and incident amplitudes:

$$A_R = A_I \quad \text{when} \quad \mathbf{n}.\nabla c = 0 \quad \text{on} \quad \partial\Omega. \tag{5.8}$$

6. Local solution

Barton (1978, § 4) points out that one important application of a short-term solution is to provide starting conditions for a subsequent numerical scheme. For this purpose the global ray solution is unnecessarily complicated, and it suffices to calculate the local solution near the centre of the contaminant cloud.

For large Péclet numbers it may be necessary to follow the contaminant cloud for a substantial distance before it becomes large enough to be resolved by a numerical scheme. Thus we transfer the origin of our Cartesian co-ordinate system to the fluid element at the centre of the cloud:

$$\hat{\mathbf{x}} = \mathbf{x}-\int_0^s u_0(\tau)\,d\tau, \quad \hat{\mathbf{r}} = \mathbf{R}-\mathbf{u}. \tag{6.1}$$

Next, instead of the full ray-tracing equations (3.2), (3.5) and (3. 3), we solve the linear approximations

$$d\hat{x}_i/ds = \hat{r}_i + (\partial u_i/\partial x_j)\hat{x}_j, \tag{6.2a}$$

$$d\hat{r}_i/ds = -(\partial u_j/\partial x_i)\hat{r}_j, \tag{6.2b}$$

$$\partial\phi/ds = -\hat{r}_i\hat{r}_i/4\kappa. \tag{6.2c}$$

Here the rate-of-strain matrix $(\partial u_i/\partial x_j)$ is a function of the time of travel s along the flow path.

To write the solutions in compact form we introduce the distortion matrix E and its inverse E^{-1}:

$$dE_{ij}/ds = -(\partial u_i/\partial x_k)E_{kj}, \tag{6.3a}$$

$$d(E^{-1})_{ij}/ds = (\partial u_i/\partial x_k)(E^{-1})_{kj}, \tag{6.3b}$$

with

$$E(0)_{ij} = E^{-1}(0)_{ij} = \delta_{ij}. \tag{6.3c}$$

The corresponding solutions of the linearized equations (6.2) are

$$\hat{x}_i = (E^{-1})_{il}(s)\int_0^s E_{lk}(\tau)\,E_{jk}(\tau)\,d\tau\,\hat{r}_j(0), \tag{6.4a}$$

$$\hat{r}_i = E_{ji}(s)\hat{r}_j(0), \tag{6.4b}$$

$$\phi = -\frac{1}{4\kappa}\hat{r}_i(0)\hat{r}_k(0)\int_0^s E_{ij}(\tau)\,E_{kj}(\tau)\,d\tau. \tag{6.4c}$$

To evaluate the ray separation (4.2), we must differentiate $\hat{x}_i$ with respect to $\hat{r}_j(0)$ and then take the determinant

$$J = \det\left[(E^{-1})_{il}\int_0^s E_{lk}(\tau)\,E_{jk}(\tau)\,d\tau\right]. \tag{6.5}$$

Since there is a linear relationship between $\hat{x}_i$ and $\hat{r}_j(0)$ we can infer that the decay exponent ϕ is a homogeneous quadratic. Equivalently, the shape of the contaminant cloud evolves from its initial spherical shape into an ellipsoid. This local result is confirmed in the next two sections when we construct the global ray solutions. An exceptional case is when $\partial u_i/\partial x_j$ is locally zero, and the contaminant cloud remains spherical until it is reasonably large (see figure 8 below).

7. A source near a stagnation point

Chatwin (1974) gives an explicit solution for a discharge released from an arbitrary position x_0, y_0 in an irrotational flow

$$\mathbf{u} = (lx, -ly, 0), \tag{7.1}$$

with an impermeable boundary along the streamline $y = 0$ (see figure 3).

In the ray method the first task is to determine the (two-dimensional) ray paths

$$dt/ds = 1, \quad d\mathbf{x}/ds = \mathbf{R}, \quad d\mathbf{R}/ds = l^2\mathbf{x}, \tag{7.2}$$

(equations (3.2), (3.5)). The solution can be written as a two-parameter family:

$$x = x_0 e^{ls} + p\sinh ls, \quad y = y_0 e^{-ls} + q\sinh ls, \tag{7.3a, b}$$

$$R_1 = lx + lpe^{-ls}, \qquad R_2 = -ly + lqe^{ls}, \tag{7.3c, d}$$

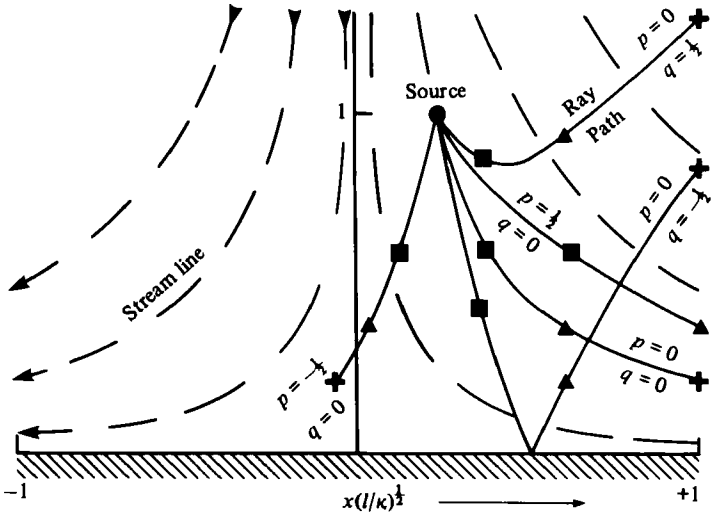

FIGURE 3. Streamlines and ray paths for flow near a stagnation point. ●, $ls = 0$; ■, $ls = 0{\cdot}5$; ▲, $ls = 1$; +, $ls = 1{\cdot}5$.

where lp, lq are the initial components of the vector $\mathbf{R}-\mathbf{u}$. For negative q, the rays intersect the boundary and the reflected rays are given by

$$y = -y_0 e^{-ls} - q\sinh ls, \quad R_2 = -ly - lqe^{ls}, \tag{7.4a, b}$$

together with the formulae for x and R_1 unchanged.

Along both families of rays the equation (3.3) for the decay exponent has the solution

$$\phi = -[p^2(1-e^{-2ls}) + q^2(e^{2ls}-1)]/8\kappa. \tag{7.5}$$

Also, the Jacobian (4.2) for the ray separation has the value

$$J = \sinh^2 ls. \tag{7.6}$$

Thus, from (4.9), with $n = 2$, we find that the amplitude factor is given by

$$A_I = A_R = Pl/4\pi\kappa \sinh ls. \tag{7.7}$$

To translate our solution back from ray variables (p, q, s) to physical variables (x, y, t), we invert (7.3) and (7.4):

$$s = t, \quad p = 2e^{lt}(x - x_0 e^{lt})/(e^{2lt}-1), \tag{7.8a, b}$$

$$q_I = 2e^{-lt}(y - y_0 e^{-lt})/(1-e^{-lt}), \tag{7.8c}$$

$$q_R = -2e^{-lt}(y + y_0 e^{-lt})/(1-e^{-lt}). \tag{7.8d}$$

Adding together the incident and reflected ray solutions we obtain

$$c = \frac{Pl}{4\pi\kappa \sinh lt} \exp\left[-\frac{Pl(x-x_0e^{lt})^2}{2\kappa(e^{2lt}-1)}\right] \times \left\{\exp\left[-\frac{Pl(y-y_0e^{-lt})^2}{2\kappa(1-e^{-2lt})}\right] + \exp\left[-\frac{Pl(y+y_0e^{-lt})^2}{2\kappa(1-e^{-2lt})}\right]\right\}. \tag{7.9}$$

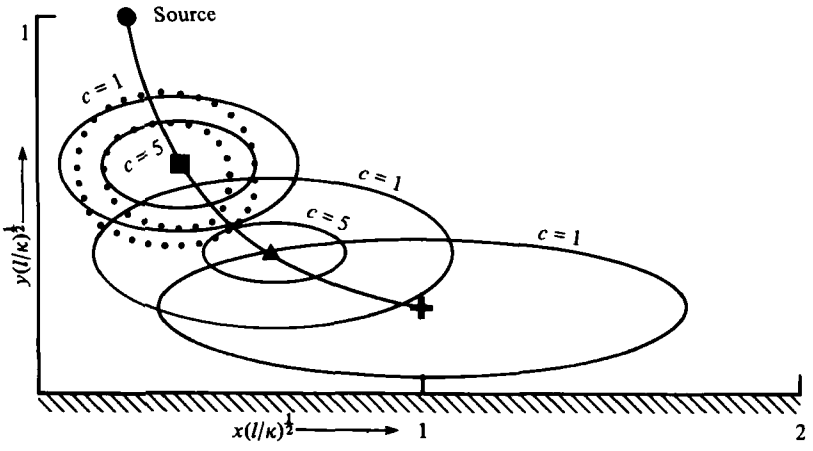

FIGURE 4. Concentration contours for a point release of contaminant in a stagnation flow.

This is identical to the solution given by Chatwin (1974). Thus, it happens that in this case the ray solution is exact rather than being an asymptotic approximation valid for large P. By contrast, the Taylor series expansion derived by Barton (1978, § 4) is useful only for $lt < 0{\cdot}2$ (i.e. the time during which the curvature of the streamlines can be neglected).

For illustrative purposes figure 4 shows concentration contours at times $lt = 0{\cdot}5, 1, 1{\cdot}5$ for a stagnation flow with Péclet number $P = 100$. The effect of the shear distortion is to elongate the contaminant cloud in the x-direction. For the earliest of the three times, the dotted contours confirm that Barton's three-term series approximation is already beyond its range of validity.

8. Initial dispersion near a point vortex

Following Barton (1978), we take as our second example the flow near a point vortex. In polar co-ordinates the velocity field is

$$\mathbf{u} = (0, \alpha/r, 0). \tag{8.1}$$

The two-dimensional ray-tracing equations (3.2) and (3.5) take the form

$$\frac{dt}{ds} = 1, \quad \frac{dr}{ds} = R_1, \quad r\frac{d\theta}{ds} = R_2, \tag{8.2a, b, c}$$

$$\frac{dR_1}{ds} - \frac{d\theta}{ds}R_2 = -\frac{\alpha^2}{r^3}, \quad \frac{dR_2}{ds} + R_1\frac{d\theta}{ds} = 0. \tag{8.2d, e}$$

(Note the additional terms which arise owing to the changing orientation of the co-ordinate direction as θ varies.) In the θ-direction there is conservation of angular momentum along rays:

$$d\theta/ds = \alpha q/r^2, \tag{8.3}$$

where q is a ray parameter. The solution in the radial direction is

$$r = [r_0^2 + 2\alpha ps + \alpha^2(q^2 - 1)\, s^2/r_0^2]^{\frac{1}{2}}. \tag{8.4}$$

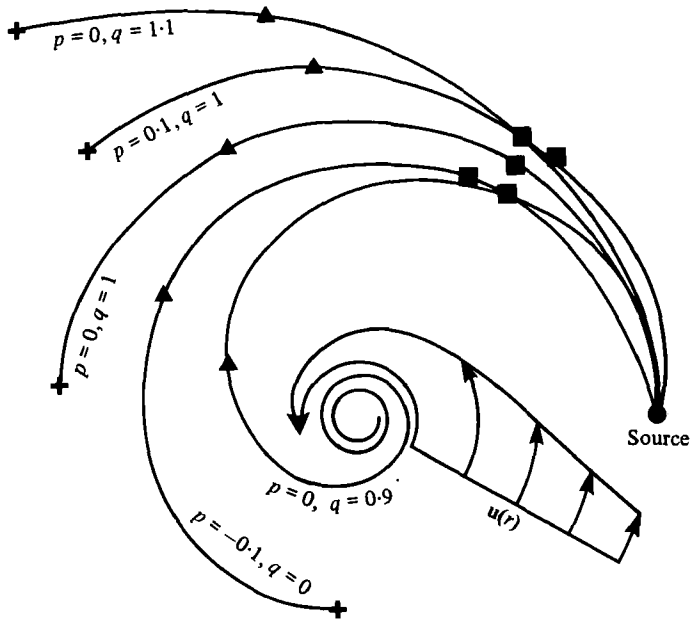

FIGURE 5. Velocity profile and ray paths for flow near a point vortex.
●, $\alpha t/r_0^2 = 0$; ■, $\alpha t/r_0^2 = 1$; ▲, $\alpha t/r_0^2 = 2$; +, $\alpha t/r_0^2 = 3$.

Thus, if the values of the ray parameters p, q are such that either $q^2 < 1$ or $p < -[q^2-1]^{\frac{1}{2}}$ then the rays eventually go through the eye of the vortex (see figure 5).

Strictly, the solution for θ has two different branches depending upon the sign of p^2+1-q^2. However, it is mathematically convenient to combine these into the single expression:

$$\theta-\theta_0 = \frac{q}{\{p^2+1-q^2\}^{\frac{1}{2}}}\,\tfrac{1}{2}\ln\left[\frac{1+(\alpha s/r_0^2)\,(p+\{p^2+1-q^2\}^{\frac{1}{2}})}{1+(\alpha s/r_0^2)\,(p-\{p^2+1-q^2\}^{\frac{1}{2}})}\right], \tag{8.5}$$

where any logarithms of complex argument can be re-expressed in terms of arctangents. We note that there is a logarithmic singularity in θ for those rays which approach the vortex (i.e. the rays spiral faster and faster near the origin). Thus a local analysis of this region would be required if we wished to extend the rays across the singularity.

Substituting the above results (8.4) and (8.5) for the ray paths into (3.3), we find that the decay exponent ϕ is given by

$$-4\frac{\kappa}{\alpha}\phi = \frac{(2-2q+p^2)}{\{p^2+1-q^2\}^{\frac{1}{2}}}\,\tfrac{1}{2}\ln\left[\frac{1+(\alpha s/r_0^2)\,(p+\{p^2+1-q^2\}^{\frac{1}{2}})}{1+(\alpha s/r_0^2)\,(p-\{p^2+1-q^2\}^{\frac{1}{2}})}\right]+(q^2-1)\,(\alpha s/r_0^2). \tag{8.6}$$

Similarly, the Jacobian (4.2) for the ray separation can be written as

$$\begin{aligned} J &= r\,\partial(r,\theta)/\partial(p,q) \\ &= (\alpha s/r_0^2)\frac{(p^2+1+pq^2(\alpha s/r_0^2))}{\{p^2+1-q^2\}^{\frac{3}{2}}}\,\tfrac{1}{2}\ln\left[\frac{1+(\alpha s/r_0^2)\,(p+\{p^2+1-q^2\}^{\frac{1}{2}})}{1+(\alpha s/r_0^2)\,(p-\{p^2+1-q^2\}^{\frac{1}{2}})}\right]-\frac{q^2(\alpha s/r_0^2)^2}{p^2+1-q^2}. \end{aligned} \tag{8.7}$$

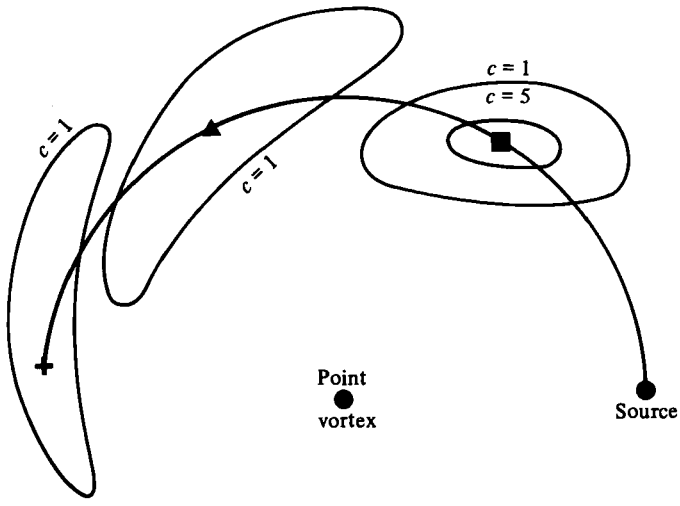

FIGURE 6. Concentration contours for a point release in a two-dimensional vortex flow.

In particular, if we set $q = 1$ and take the limit as p tends to zero, we find that, at the centre of the contaminant cloud,

$$\phi = 0 \quad \text{and} \quad J = (\alpha s/r_0^2)^2 + \tfrac{1}{3}(\alpha s/r_0^2)^4. \tag{8.8}$$

Thus, for small times, the peak concentration decays following the diffusion-equation result,

$$A \sim P/4\pi\kappa t, \tag{8.9}$$

but at large times the effect of the shear leads to a much more rapid decay rate:

$$A \sim P3^{\frac{1}{2}} r_0^2/4\pi\kappa\alpha t^2. \tag{8.10}$$

By neglecting the transmission of rays across the vortex, the present theory is restricted to times less than that required for a significant amount of contaminant to diffuse towards the vortex. Close to the origin we can use (8.4) to eliminate p in favour of q. Thus, from (8.6) we find that the dominant (singular) contribution to the decay exponent is given by

$$\phi = [\{1 + (q^2-1)^2 (\alpha s/r_0^2)^4\}^{\frac{1}{2}} + 4(\alpha s/r_0^2)^2 (q-1)^2 \{1 + (q^2-1)^2 (\alpha s/r_0^2)^4\}^{-\frac{1}{2}}] \times (r_0^2/8\kappa s) \ln (r^2/r_0^2). \tag{8.11}$$

This has a minimum at $q = 1$, with the value

$$\phi = (r_0^2/8\kappa s) \ln (r^2/r_0^2). \tag{8.12}$$

Hence a sufficient condition for the applicability of the present theory is that

$$s = t < Pr_0^2/8\kappa. \tag{8.13}$$

Since the Péclet number P is assumed to be large, this is much less stringent than the upper bound $0{\cdot}15r_0^2/\alpha$ for the validity of Barton's (1978) analysis.

Figure 6 shows concentration contours at times $\alpha t/r_0^2 = 1, 2, 3$ in a vortex flow with Péclet number $P = 100$. As is also apparent in Barton's figure 2, the concentration contours tend to drift outwards and do not merely follow the particle paths. The ray

interpretation of this feature is that the rays, and hence the contaminant flux, tend to be strongest towards the origin. Thus, the erosion of concentration is greatest at the inside, giving the illusion of the contaminant distribution drifting outwards. The local solution derived in § 6 would suggest that the concentration cloud should initially be elliptical with principal axes inclined at 45 degrees to the flow direction. This is in good agreement with the results at the earliest of the three times. However, there are substantial banana-like distortions when the contaminant cloud becomes large.

9. Initial dispersion in plane Poiseuille flow

As our final example we again follow Barton (1978) and investigate plane Poiseuille flow:

$$\mathbf{u} = \bar{u}(\tfrac{3}{2} - \tfrac{3}{2}(y/b)^2, 0, 0), \quad -b < y < b, \tag{9.1}$$

where $\bar{u}$ is the bulk velocity, and $2b$ is the separation between the rigid impermeable walls.

The ray equations (3.2) and (3.5) take the form

$$\frac{dt}{ds} = 1, \quad \frac{dx}{ds} = R_1, \quad \frac{dy}{ds} = R_2, \tag{9.2a, b, c}$$

$$\frac{dR_1}{ds} = -3\frac{\bar{u}}{b} R_2\left(\frac{y}{b}\right), \quad \frac{dR_2}{ds} = \frac{9\bar{u}^2}{2b}\left[\left(\frac{y}{b}\right)^3 - \left(\frac{y}{b}\right)\right] + \frac{3\bar{u}}{b} R_1\left(\frac{y}{b}\right). \tag{9.2d, e}$$

The equation for R_1 can be integrated to give the neat result

$$R_1 - u_1(y) = p\bar{u} = \text{constant along rays.} \tag{9.3}$$

Thus, in the longitudinal direction the ray velocity differs from the local velocity by a fixed amount. Moreover, this discrepancy is unchanged upon reflection of the rays at the two boundaries.

From the R_2 equation we now find that the ray position across the flow satisfies the constant coefficient ordinary differential equation

$$d^2y/ds^2 - 3p(\bar{u}/b)^2 y = 0. \tag{9.4}$$

Thus, the solution is hyperbolic or trigonometric according as the rays move faster or slower than the local current. When we take into account the reflection at boundaries, we find that for $p > 0$ the solution can be written

$$y = y_0 \cosh\zeta + bq \sinh\zeta/(3p)^{\frac{1}{2}}, \tag{9.5a}$$

with

$$\zeta = (3p)^{\frac{1}{2}}(\bar{u}s/b) - m\Delta. \tag{9.5b}$$

Here q is a ray parameter, the integer m counts the number of times that the ray has been reflected at the boundaries, and the periodicity Δ is defined by

$$\sinh\Delta = 2\left\{1 + \frac{q^2}{3p} - \left(\frac{y_0}{b}\right)^2\right\}^{\frac{1}{2}} \Big/ \left|\frac{q^2}{3p} - \left(\frac{y_0}{b}\right)^2\right|. \tag{9.6}$$

For $p < 0$ the solution is the analytic continuation of equations (9.5), (9.6) with cosh and sinh replaced by their trigonometric counterparts. An important difference is that in the parameter range

$$q^2 < -3p(1-(y_0/b)^2), \tag{9.7}$$

the rays never reach the boundary. Thus, there is total internal reflection and we can set $m = 0$.

Integrating the equation $dx/ds = R_1$, we find that the ray position along the flow is given by

$$x - x_0 = \bar{u}s\left[p + \frac{3}{2} - \frac{3}{4}\left(\frac{y_0}{b}\right)^2 + \frac{q^2}{4p}\right] - \frac{3}{2}\frac{mb}{(3p)^{\frac{1}{2}}}\left\{1 + \frac{q^2}{3p} - \left(\frac{y_0}{b}\right)^2\right\}^{\frac{1}{2}}$$
$$- b\left[\frac{3}{4}\left(\frac{y_0}{b}\right)^2 + \frac{q^2}{4p}\right]\frac{\sinh 2\zeta}{2(3p)^{\frac{1}{2}}} - \tfrac{3}{2}y_0 q\left[\frac{\cosh 2\zeta - 1}{6p}\right]. \tag{9.8}$$

We note that the definition (9.6) of the periodicity with respect to ζ makes it possible for us to eliminate the reflection number m in favour of the time parameter s.

The geometry of the ray paths (see figure 7) can be understood by reference to the general principles noted in § 3. The flow velocity is greatest along the centre line, and the vorticity is anti-clockwise or clockwise according as y/b is positive or negative. For rays with **R** small (i.e., p negative and q small) the dominant influence upon the ray curvature is the tendency to bend towards the region of strongest current. This describes the sinuous rays which undergo total internal reflection (see figure 7(i)). Then, as **R** gets larger, the rays tend to rotate in the same sense as the vorticity. For backward-moving rays, with p negative, this again implies that the rays curve back towards the centre-line (figure 7(ii)). However, for forward-moving rays, the same sense of rotation has the opposite effect and leads to rays which curve away from the centre line (figure 7(iii)). Finally, if the cross-stream component of the ray velocity **R** is sufficiently large, then we get rays which manage to cross between the boundaries despite the opposing curvature (figure 7(iv)).

From the eikonal equation (3.3), we find that the decay exponent ϕ can be written

$$\phi = -\frac{\bar{u}^2 s}{4\kappa}\left[p^2 + \tfrac{1}{2}q^2 - \tfrac{3}{2}p\left(\frac{y_0}{b}\right)^2\right] - \frac{3}{4}\frac{m\bar{u}b}{\kappa}p\left\{1 + \frac{q^2}{3p} - \left(\frac{y_0}{b}\right)^2\right\}^{\frac{1}{2}}$$
$$- \frac{b\bar{u}}{2\kappa}p\left[\frac{3}{4}\left(\frac{y_0}{b}\right)^2 + \frac{q^2}{4p}\right]\frac{\sinh 2\zeta}{2(3p)^{\frac{1}{2}}} - \frac{3\bar{u}}{4\kappa}y_0 qp\left[\frac{\cosh 2\zeta - 1}{6p}\right]$$
$$= \frac{p\bar{u}}{2\kappa}\left\{(x - x_0) - \tfrac{3}{2}\bar{u}s\left[1 + p - \left(\frac{y_0}{b}\right)^2 + \frac{q^2}{3p}\right]\right\}. \tag{9.9}$$

(i.e. exponential decay with respect to distance in axes moving at constant velocity.)

For $m = 0$ the Jacobian (4.2) for the ray separation is given by the formula

$$J = b^2\frac{\zeta\sinh\zeta}{3p} + \frac{3}{16}\frac{y_0^2}{p}\frac{\sinh\zeta[\sinh 2\zeta - 2\zeta]}{3p}$$
$$+ \frac{b^2}{16}\frac{q^2}{p^2}\frac{[\sinh 2\zeta\sinh\zeta + 2\zeta\sinh\zeta - 4\zeta^2\cosh\zeta]}{3p}$$
$$+ \frac{3}{8}\frac{y_0 bq}{p}\frac{\sinh\zeta[\cosh 2\zeta - 1 - 2\zeta^2]}{(3p)^{\frac{3}{2}}}. \tag{9.10}$$

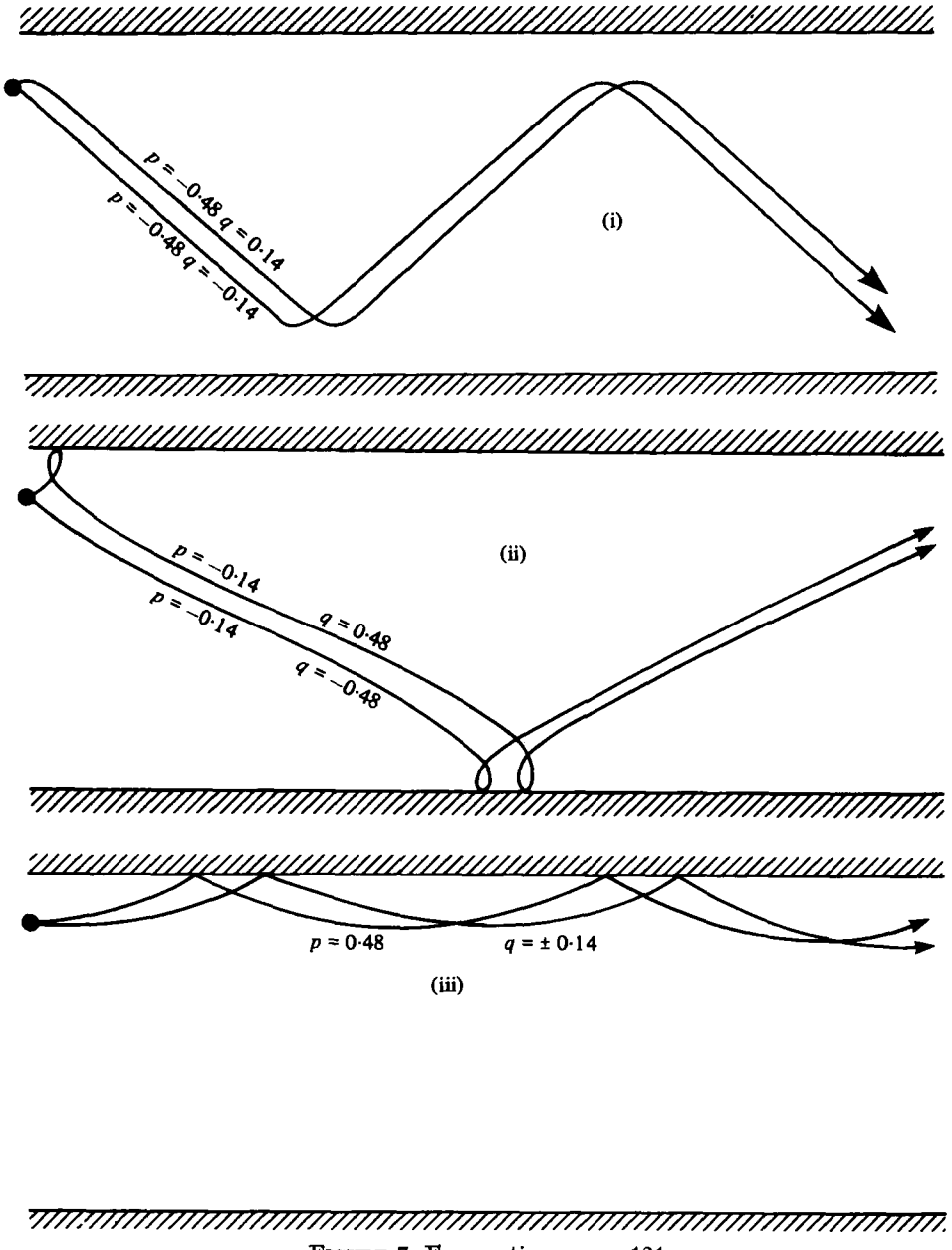

FIGURE 7. For caption see p. 121.

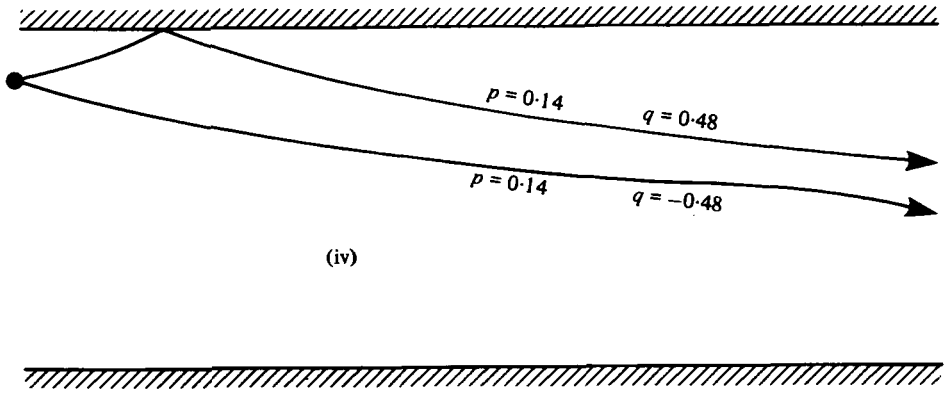

FIGURE 7. The variety of ray paths for plane Poiseuille flow.

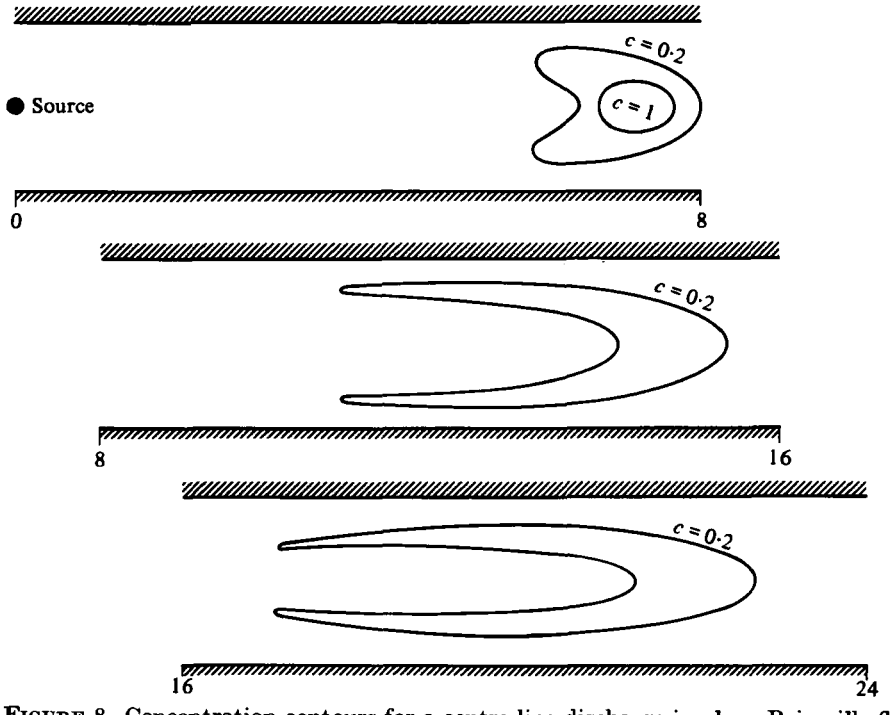

FIGURE 8. Concentration contours for a centre-line discharge in plane Poiseuille flow.

Although J is continuous at reflection, the explicit formula for $m > 0$ is extremely lengthy and, consequently, is omitted here. We note that as p and q tend to zero,

$$\phi \sim 0 \quad \text{and} \quad J \sim \bar{u}^2 s^2 \left[1 + \frac{3}{4}\left(\frac{\bar{u} s y_0}{b^2}\right)^2\right]. \tag{9.11}$$

Thus, as was the case in the previous example, the local velocity shear leads to a transition from t^{-1} to a t^{-2} decay law for the peak amplitude:

$$A \sim P/4\pi\kappa t \left[1 + \frac{3}{4}\left(\frac{\bar{u} t y_0}{b^2}\right)^2\right]^{\frac{1}{2}}. \tag{9.12}$$

Figure 8 shows concentration contours at times $\bar{u}t/b = 5, 10, 15$ for a centre-line discharge in plane Poiseuille flow with Péclet number $P = 100$. For this particular discharge site, the amount of shear experienced across the contaminant grows as t, rather than the more usual $t^{\frac{1}{2}}$ result. Thus the shear distortion is imperceptible until comparatively large times and then grows very rapidly. The persistence of the contaminant at the centre of the flow is exaggerated by the strong dilution caused by the velocity shear far from the centre line. As in all the previous examples, these results are at times an order of magnitude beyond the range of validity of the methods used by Chatwin (1976, 1977) and by Barton (1978).

This work was supported by B.P. through the award of the Royal Society British Petroleum Company Limited Senior Research Fellowship.

REFERENCES

BARTON, N. G. 1978 The initial dispersion of soluble matter in three-dimensional flow. *J. Austral Math. Soc.* B **20**, 265–279.

CARO, C. G. 1966 The dispersion of indicator flowing through simplified models of the circulation and its relevance to velocity profile in blood vessels. *J. Physiol.* **185**, 501–519.

CHATWIN, P. C. 1974 The dispersion of contaminants released from instantaneous sources in laminar flow near stagnation points. *J. Fluid Mech.* **66**, 753–766.

CHATWIN, P. C. 1976 The initial dispersion of contaminant in Poiseuille flow and the smoothing of the snout. *J. Fluid Mech.* **77**, 593–602.

CHATWIN, P. C. 1977 The initial development of longitudinal dispersion in straight tubes. *J. Fluid Mech.* **80**, 33–48.

COHEN, J. K., HAGIN, F. G. & KELLER, J. B. 1972 Short-time asymptotic solutions of parabolic equations. *J. Math. Anal. Applic.* **38**, 83–91.

COHEN, J. K. & LEWIS, R. M. 1967 A ray method for the asymptotic solution of the diffusion equation. *J. Inst. Math. Applic.* **3**, 266–290.

COURANT, R. & HILBERT, D. 1962 *Methods of Mathematical Physics*, vol. 2. Interscience.

GILL, W. N. & SANKARASUBRAMANIAN, R. 1970 Exact analysis of unsteady convective diffusion. *Proc. Roy. Soc.* A **316**, 341–350.

LIGHTHILL, M. J. 1966 Initial development of diffusion in Poiseuille flow. *J. Inst. Math. Applic.* **2**, 97–108.

MCQUIVEY, R. S. & KEEFER, T. N. 1976*a* Convective model of longitudinal dispersion. *J. Hydraulics Div. A.S.C.E.* **102**, 1409–1424.

MCQUIVEY, R. S. & KEEFER, T. N. 1976*b* Dispersion – Mississippi River below Baton Rouge, La. *J. Hydraulics Div. A.S.C.E.* **102**, 1425–1437.

SMITH, R. 1981 A delay-diffusion description for contaminant dispersion. *J. Fluid Mech.* **105**, 469–486.

TAYLOR, G. I. 1953 Dispersion of soluble matter in solvent flowing slowly through a tube. *Proc. Roy. Soc.* A **219**, 186–203.

TAYLOR, G. I. 1954 The dispersion of matter in turbulent flow through a pipe. *Proc. Roy. Soc.* A **223**, 446–468.

TOWNSEND, A. A. 1951 The diffusion of heat spots in isotropic turbulence. *Proc. Roy. Soc.* A **209**, 418–430.